Dalton Transactions

PAPER

View Article Online
View Journal | View Issue

Cite this: *Dalton Trans.*, 2014, **43**, 8241

Synthesis and characterisation of the complete series of B–N analogues of triptycene†

Ömer Seven, Sebastian Popp, Michael Bolte, Hans-Wolfram Lerner and Matthias Wagner*

The reaction between the bisborate $Li_2[o\text{-}C_6H_4(BH_3)_2]$ and 2 equivalents of an appropriate pyrazole derivative (Hpz^R) in the presence of Me_3SiCl yields *o*-phenylene-bridged pyrazaboles $HB(\mu\text{-}pz^R)_2(\mu\text{-}o\text{-}C_6H_4)BH$ (**3a–3e**; Hpz^R = 4-iodopyrazole (**3a**), 4-(trimethylsilyl)pyrazole (**3b**), 3,5-dimethylpyrazole (**3c**), 3,5-di(*tert*-butyl)pyrazole (**3d**), 3,5-bis(trifluoromethyl)pyrazole (**3e**)). The synthesis approach thus provides access to uncharged B–N triptycenes bearing (i) functionalisable groups, (ii) electron-donating or -withdrawing substituents and (iii) pyrazole rings of varying steric demand. Treatment of $p\text{-R*}C_6H_4BBr_2$ with the potassium tris(pyrazol-1-yl)borates $K[HBpz_3]$ or $K[p\text{-R*}C_6H_4Bpz_3]$ yields cationic pyrazolyl-bridged pyrazaboles $[p\text{-}BrC_6H_4B(\mu\text{-}pz)_3BH]Br$ ([**4a**]Br) and $[p\text{-R*}C_6H_4B(\mu\text{-}pz)_3Bp\text{-}C_6H_4R^*]Br$ (R* = Br ([**4b**]Br), I ([**4c**]Br), $SiMe_3$ ([**4d**]Br)), which can be regarded as full B–N analogues of triptycene. The B–H bonds of **3b** and [**4a**]Br are unreactive towards *t*BuC≡CH even at temperatures of 80 °C, thereby indicating an appreciable thermal stability of the corresponding B–N cage bonds. Most of the cage compounds are sufficiently inert towards water to allow quick aqueous workup. However, NMR spectroscopy in CD_3OD solution reveals degradation of **3b** or [**4a**]Br to the corresponding pyrazoles and $o\text{-}C_6H_4(B(OCD_3)_2)_2$ or $p\text{-}BrC_6H_4B(OCD_3)_2/B(OCD_3)_3$. The diphenylated species [**4b**]Br is significantly more stable under the same measurement conditions; even after 76 d, most of the material degrades only to the stage of the *syn*/*anti*-pyrazaboles $p\text{-}BrC_6H_4(CD_3O)B(\mu\text{-}pz)_2B(OCD_3)p\text{-}C_6H_4Br$ (**11a**/**11b**). A derivatisation of [**4c**]Br with $n Bu_3SnC{\equiv}Ct Bu$ through Stille-type coupling reactions furnishes the alkynyl derivative $[p\text{-}t BuC{\equiv}CC_6H_4B(\mu\text{-}pz)_3Bp\text{-}C_6H_4C{\equiv}Ct Bu]Br$ ([**4e**]Br). Larger B–N aggregates are also accessible: treatment of the tetrakisborate $Li_4[1,2,4,5\text{-}C_6H_2(BH_3)_4]$ with 4 equivalents of $HpzR$ in the presence of Me_3SiCl leads to the corresponding B–N pentiptycenes **14a–14d** ($HpzR$ = 3,5-bis(trifluoromethyl)pyrazole (**14a**), 4-(trimethylsilyl)pyrazole (**14b**), 3,5-dimethylpyrazole (**14c**), 3,5-di(*tert*-butyl)pyrazole (**14d**)).

Received 11th February 2014,
Accepted 25th February 2014

DOI: 10.1039/c4dt00442f

www.rsc.org/dalton

Introduction

Triptycenes **1** (Fig. 1) are a class of organic compounds possessing a three-dimensional paddle-wheel structure. Due to their rigid bicyclo[2.2.2]octatriene core, angles close to 120° are maintained between the three *o*-phenylene ring panels, which leads to the formation of three equally sized compartments lined with π-electron clouds. On the one hand, this unique geometry often frustrates space-efficient packing and thereby leads to void spaces in a supramolecular assembly, called the "internal free volume" (IFV), which can be used to store small guest molecules.[1] On the other hand, the three triptycene blades have also been used to create interlocking molecular structures acting as rotors, gearings or brakes in molecular machines.[2,3] Triptycenes are therefore useful building blocks for the generation of sophisticated molecular architectures with well-defined geometries.[4] During the last few decades, a wide spectrum of applications has opened up, ranging from materials[5,6] and sensor science[7] to host–guest[5,8] and coordination chemistry.[4,9]

Further developments in these fields are critically dependent on the availability of broadly functionalised triptycene derivatives. To date, the Diels–Alder reactions between anthracenes and *p*-benzoquinones or benzynes have offered the most important methods for the assembly of triptycene scaffolds (Scheme 1). With respect to functional-group compatibility, it is therefore essential to be able to release benzyne intermediates *in situ* under mild conditions and with high efficiency;

Institut für Anorganische Chemie, J.W. Goethe-Universität Frankfurt, Max-von-Laue-Strasse 7, D-60438 Frankfurt (Main), Germany.
E-mail: Matthias.Wagner@chemie.uni-frankfurt.de

†Electronic supplementary information (ESI) available: Experimental details including assigned NMR data of **3c**, **3d**, **3e**, K[**8**] (R = *p*-$Me_3SiC_6H_4$; *p*-IC_6H_4), **14c** and **14d**. Plots of the $^{13}C\{^1H\}$ NMR spectra of **3a**, **3c**, **3d**, [**4a**]Br, [**4c**]Br, [**4e**]Br, **14b**, **14c** and **14d**. Decomposition experiments of **3b**, [**4a**]Br and [**4b**]Br in CD_3OD and [**4d**]Br in CH_3OH. X-ray crystal structure analyses of **3c**, **3d**, **3e**, **3f**·OEt_2 and **12a**. CCDC 985503–985515. For ESI and crystallographic data in CIF or other electronic format see DOI: 10.1039/c4dt00442f

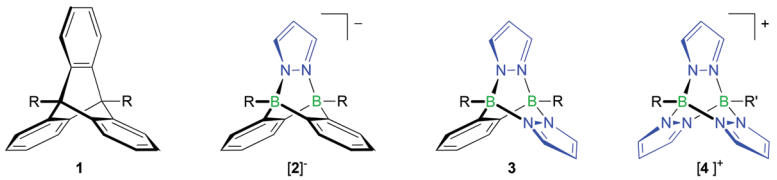

Fig. 1 Triptycene (**1**) and its B–N analogues $[\mathbf{2}]^-$, **3** and $[\mathbf{4}]^+$.

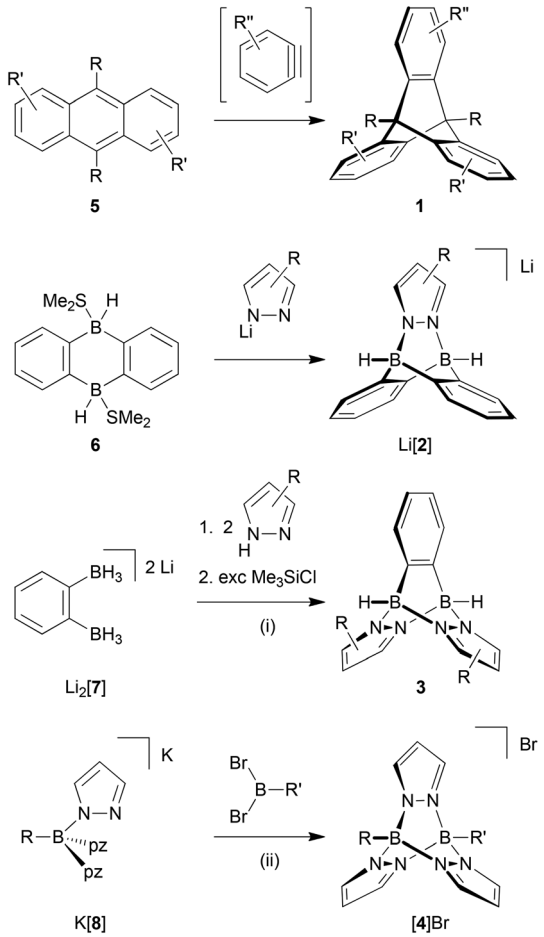

Scheme 1 General synthesis methods of all-carbon triptycenes and of the complete series of B–N triptycenes. General reaction conditions: (i) Et_2O, rt, between 12 h and 15 h. (ii) CH_3CN-toluene or toluene, between rt and 120 °C, between 8 h and 24 h.

good results are usually obtained through aprotic diazotisation of anthranilic acids with amyl nitrite[10] or upon treatment of (phenyl)[2-(trimethylsilyl)phenyl]iodonium triflate with an appropriate fluoride source.[11] Even though various halogenated 1,2-bis(trimethylsilyl)benzenes have recently been made available,[12] which are suitable starting materials for the synthesis of corresponding halogenated hypervalent iodine benzyne precursors, the crucial role of the benzyne intermediates in triptycene syntheses still constitutes a bottleneck on the way to novel triptycene-containing functional units.

Our group has a long-standing interest in exploiting the B–N/C–C isosterism for the facile synthesis of complex molecular frameworks.[13–16] This approach takes advantage of the fact that B–N adduct bonds tend to form spontaneously in essentially quantitative yields whereas the isoelectronic C–C single bonds are usually much harder to establish.[17,18] The general concept of B–N/C–C isosterism is very well applicable for the preparation of triptycene analogues (*cf.* compounds $[\mathbf{2}]^-$, **3** and $[\mathbf{4}]^+$; Fig. 1).

In a previous communication, we have already reported on the reaction between the Me_2S adduct of 9,10-dihydro-9,10-diboraanthracene (**6**; Scheme 1) and pyridazine, which gives a soluble B–N congener of triptycene.[19] The synthesis approach also works faithfully for phthalazine (benzo[*d*]pyridazine) or *B*-substituted 9,10-dihydro-9,10-diboraanthracenes as the starting materials. If lithium pyrazolides are used instead of pyridazine, ionic compounds of type Li[**2**] are obtained (Scheme 1; Fig. 1).[19]

While the third member of the family of B–N triptycenes, compound **3** (Fig. 1), has been unknown, scattered reports of cationic $[\mathbf{4}]^+$-type species can be found in the literature. Most of the times, the latter molecules have been observed as side products of the complexation of Lewis-acidic transition metal ions with tris(pyrazol-1-yl)borate ligands.[20] Two early reports of targeted syntheses do, however, also exist: Trofimenko prepared $[\mathbf{4}]PF_6$ (R = R′ = Et) in yields of 22% through the reaction of pyrazolide ions with $EtB(OTos)_2$ and subsequent salt metathesis (HOTos = toluenesulfonic acid); he also mentioned the relationship between $[\mathbf{4}]^+$ and triptycene.[21] In a later report, Niedenzu *et al.* described the synthesis of derivatives of $[\mathbf{4}]^+$ carrying methyl groups at the pyrazolyl rings. The boron atoms were either equipped with one hydrogen atom each or with one hydrogen atom and one ethyl group.[22] The synthesis approach relied on the reaction of tris(pyrazol-1-yl)borate anions (*cf.* $[\mathbf{8}]^-$; Scheme 1) with trigonal boranes containing two good leaving groups.

The purpose of this paper is to provide high-yield syntheses and full characterisations of selected examples of **3**- and $[\mathbf{4}]^+$-type molecules together with compounds possessing extended B–N pentiptycene-type architectures. Special emphasis will be placed on the development of *C*-halogenated derivatives, which possess promising potential as future building blocks of (supra)molecular structures. Moreover, we will investigate and compare the stabilities of the bicyclo[2.2.2]octatriene cores of $[\mathbf{2}]^-$, **3** and $[\mathbf{4}]^+$ in order to explore the scope and limitations of these molecules as triptycene substitutes.

Results and discussion

Synthesis and NMR-spectroscopic characterisation of 3- and $[4]^+$-type molecules

Neutral **3**-type compounds were prepared from the *o*-phenylene-bridged bisborate $Li_2[7]$[23] and 2 equivalents of an appropriately substituted pyrazole (Scheme 1). The first two B–N bonds assemble spontaneously at room temperature through a Brønsted acid–base reaction with liberation of H_2. Subsequent addition of excess Me_3SiCl as a hydride scavenger creates free coordination sites at the boron centres; this leads to the formation of two intramolecular B–N adduct bonds and thereby closes the molecular cage. The synthesis protocol tolerates various degrees of steric bulk at the 3,5-positions of the pyrazolyl rings: for example, derivatives carrying hydrogen atoms (**3a**, **3b**; Fig. 2), methyl groups (**3c**) or *tert*-butyl groups (**3d**) are all formed in good yields. It is also possible to employ both electron-richer (*cf.* the H_3C-derivative **3c**) and electron-poorer pyrazoles (*cf.* the CF_3-derivative **3e**) with similar success; **3e** is, however, significantly more prone to hydrolysis than **3c**. We also found that the *o*-phenylene ring may be replaced by other (metal)organic fragments, because the synthesis sequence can also be applied to the 1,1′-ferrocenylene-bridged bisborate $Li_2[1,1'\text{-fc}(BH_3)_2]$[24,25] to give compounds like **3f** (Fig. 2). **3f** can not only be viewed as an Fe-containing B–N triptycene, but also as an *ansa*-ferrocene with pyrazabole[26] bridge.[14]

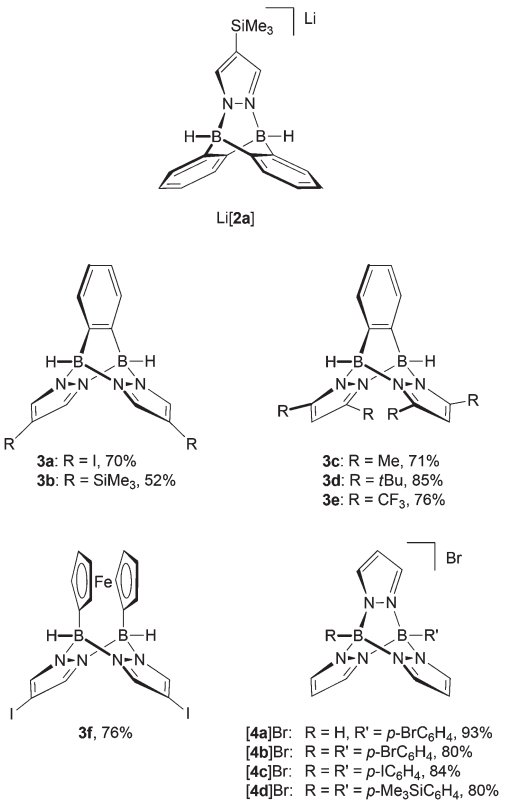

Fig. 2 Compilation of the B–N triptycenes of types $[2]^-$, **3** and $[4]^+$ discussed in this paper.

Cationic $[4]^+$-type B–N triptycenes are accessible starting from readily available potassium tris(pyrazol-1-yl)borates[27,28] (K[**8**]; *cf.* the ESI† for detailed information) and dibromo(organyl)boranes (Scheme 1). This synthesis approach provides access to unsymmetrically (R = H, R′ = *p*-BrC_6H_4 ([**4a**]Br); Fig. 2) as well as symmetrically *B*-functionalised compounds (R = R′ = *p*-BrC_6H_4 ([**4b**]Br), *p*-IC_6H_4 ([**4c**]Br) or *p*-$Me_3SiC_6H_4$ ([**4d**]Br); Fig. 2). The combination of R = R′ = (substituted) phenyl with 3,5-dimethylpyrazole generally failed to give the desired B–N triptycenes, likely due to prohibitively high steric congestion. The use of 4-bromo- or 4-iodopyrazole led to very poorly soluble products, which were hard to purify and characterise and are consequently not considered further.

The $^{11}B\{^1H\}$ NMR shifts of all the B–N triptycenes under consideration here fall in the range between 0.2 ppm and −7.0 ppm, thereby testifying to the presence of tetracoordinated boron nuclei.[29] Compound [**4a**]Br, which possesses two magnetically inequivalent boron centres, gives rise to two signals in the $^{11}B\{^1H\}$ NMR spectrum (−0.5 ppm (*B*C); −5.4 ppm (*B*H)); all other molecules show only one resonance each. B,H-coupling is resolved only in the cases of **3c** (d, $^1J_{B,H}$ = 98 Hz) and [**4a**]Br (d, $^1J_{B,H}$ = 128 Hz). In the ^1H NMR spectra, the boron-bonded hydrogen atoms give rise to very broad resonances in the interval between 5.5 ppm and 4.0 ppm; only for the signal of **3c** the expected quartet multiplicity is visible.

All the proton spectra of **3a–3e** contain two characteristic multiplets for the *o*-phenylene rings; the organometallic derivative **3f** shows two virtual triplets at 4.12 ppm and 3.22 ppm for the 1,1′-ferrocenylene backbone. For each of the molecules, the overall integral ratio between the *o*-phenylene/1,1′-ferrocenylene resonances on the one hand and the pyrazolyl signals on the other confirms the proposed 1 : 2 ratio of the two moieties in **3**-type compounds. Moreover, the number of signals in the ^1H and $^{13}C\{^1H\}$ NMR spectra is in line with the suggested symmetry of the molecular frameworks.

In the ^1H NMR spectrum of the unsymmetrically *B*-substituted cation $[4a]^+$, the pyrazolyl rings lead to two doublets with characteristic low-field shifts and small $^3J_{H,H}$ coupling constants (8.24 ppm, 8.02 ppm; 2.5 Hz) and to one high-field shifted virtual triplet (6.51 ppm). The R substituent gives the two approximate doublet resonances that are expected for AA′BB′ spin systems. On going from [**4a**]Br to the symmetrically *B*-substituted species like [**4b**]Br, the two pyrazolyl doublets become one signal of double intensity and the pyrazolyl : phenylene integral ratios change from 9 H : 4 H to 9 H : 8 H.

X-ray crystal structure analyses of B–N triptycenes

Selected crystallographic data for the structure analyses discussed in the following paragraphs are compiled in Tables 1–3. (*Note*: In a crystallographic context, we are, for reasons of simplicity, treating compounds containing deuterium atoms as if they were containing exclusively hydrogen atoms.)

The reaction providing compound **3f** is less selective than in the case of the *o*-phenylene congener **3a** and the ferrocene derivative is more sensitive to air and moisture. Thus, even though we succeeded in an NMR spectroscopic and X-ray

Table 1 Crystallographic data for **3f***·3C_6H_6, **3a** and [**4a**]Br·CH_2Cl_2

	3f*·3C_6H_6	**3a**	[**4a**]Br·CH_2Cl_2
Formula	$C_{35}H_{31}B_4Fe_2I_5N_{10}$·3 C_6H_6	$C_{12}H_{10}B_2I_2N_4$	$C_{15}H_{14}B_2Br_2N_6$·CH_2Cl_2
M_r	1615.46	485.66	544.69
Colour, shape	Orange, block	Colourless, block	Colourless, block
T [K]	173(2)	173(2)	173(2)
Radiation, λ [Å]	MoKα, 0.71073	MoKα, 0.71073	MoKα, 0.71073
Crystal system	Monoclinic	Trigonal	Orthorhombic
Space group	$P2_1/c$	$R\bar{3}$	*Pnma*
a [Å]	21.7729(16)	18.7020(7)	12.0607(5)
b [Å]	11.9678(12)	18.7020(7)	9.6544(6)
c [Å]	24.4436(18)	23.5495(9)	18.1880(8)
α [°]	90	90	90
β [°]	115.688(5)	90	90
γ [°]	90	120	90
V [Å^3]	5739.9(9)	7133.3(6)	2117.79(18)
Z	4	18	4
D_{calcd} [g cm^{-3}]	1.869	2.035	1.708
F(000)	3096	4068	1072
μ [mm^{-1}]	3.240	3.961	4.095
Crystal size [mm^3]	0.10 × 0.10 × 0.10	0.20 × 0.20 × 0.10	0.20 × 0.10 × 0.05
Rflns collected	41 538	35 425	37 320
Independent rflns (R_{int})	10 130 (0.1528)	3057 (0.0689)	2170 (0.1048)
Data/restraints/parameters	10 130/390/667	3057/0/190	2170/0/147
GOF on F^2	0.914	1.082	1.180
R_1, wR_2 [$I > 2\sigma(I)$]	0.0678, 0.0973	0.0219, 0.0531	0.0353, 0.0780
R_1, wR_2 (all data)	0.1459, 0.1167	0.0221, 0.0533	0.0383, 0.0794
Largest diff. peak and hole [e Å^{-3}]	1.494, −0.848	1.246, −0.649	0.624, −0.367

Table 2 Crystallographic data for [**4b**]Br, **14a**·3 C_7H_8 and **14b**·2 CH_2Cl_2

	[**4b**]Br	**14a**·3 C_7H_8	**14b**·2 CH_2Cl_2
Formula	$C_{21}H_{17}B_2Br_3N_6$	$C_{26}H_{10}B_4F_{24}N_8$·3 C_7H_8	$C_{30}H_{50}B_4N_8Si_4$·2 CH_2Cl_2
M_r	614.76	1210.06	848.23
Colour, shape	Colourless, block	Light brown, block	Colourless, block
T [K]	173(2)	173(2)	173(2)
Radiation, λ [Å]	MoKα, 0.71073	MoKα, 0.71073	MoKα, 0.71073
Crystal system	Triclinic	Triclinic	Triclinic
Space group	$P\bar{1}$	$P\bar{1}$	$P\bar{1}$
a [Å]	9.7625(8)	8.8267(8)	10.610(2)
b [Å]	11.1593(8)	11.3525(11)	11.003(3)
c [Å]	11.5455(9)	14.2556(14)	12.115(3)
α [°]	90.305(6)	99.583(8)	63.855(17)
β [°]	107.707(6)	106.299(7)	70.231(17)
γ [°]	106.691(6)	106.005(7)	80.803(17)
V [Å^3]	1141.79(15)	1271.1(2)	1194.7(5)
Z	2	1	1
D_{calcd} [g cm^{-3}]	1.788	1.581	1.179
F(000)	600	608	446
μ [mm^{-1}]	5.322	0.156	0.380
Crystal size [mm^3]	0.20 × 0.15 × 0.10	0.26 × 0.25 × 0.22	0.21 × 0.14 × 0.09
Rflns collected	10 831	15 695	10 352
Independent rflns (R_{int})	4185 (0.0570)	4864 (0.0645)	4202 (0.1236)
Data/restraints/parameters	4185/0/289	4864/0/397	4202/0/243
GOF on F^2	1.015	1.046	0.856
R_1, wR_2 [$I > 2\sigma(I)$]	0.0363, 0.0872	0.0451, 0.1127	0.0774, 0.1452
R_1, wR_2 (all data)	0.0474, 0.0911	0.0580, 0.1189	0.1890, 0.1809
Largest diff. peak and hole [e Å^{-3}]	0.596, −0.721	0.262, −0.265	0.681, −0.406

crystallographic characterisation of **3f**, we have not been able to isolate the compound in an analytically pure form (*cf.* the ESI† for a plot of the molecular structure, which revealed no significant differences compared to other pyrazabole-bridged *ansa*-ferrocenes[14]). In two instances, single crystals of a side product/decomposition product of **3f** grew upon prolonged storage of an NMR tube containing a solution of crude **3f** in C_6D_6. X-ray crystallography revealed a neutral dinuclear ferrocene species (**3f***; Fig. 3) containing 1 pyrazole ligand, 4 pyrazolyl moieties and 4 B–H bonds. As a remarkable feature of this side product, we note that the interannular bridge of each of the two ferrocene fragments consists of one pyrazolyl ring

Table 3 Crystallographic data for **11a** and **11b**

	11a	**11b**
Formula	$C_{20}H_{20}B_2Br_2N_4O_2$	$C_{20}H_{20}B_2Br_2N_4O_2$
M_r	529.84	529.84
Colour, shape	Colourless, block	Colourless, plate
T [K]	173(2)	173(2)
Radiation, λ [Å]	MoKα, 0.71073	MoKα, 0.71073
Crystal system	Monoclinic	Monoclinic
Space group	$P2_1/c$	$P2_1/n$
a [Å]	15.7852(7)	7.6702(5)
b [Å]	22.9613(10)	12.4132(7)
c [Å]	12.9046(5)	11.2406(7)
α [°]	90	90
β [°]	113.391(3)	102.351(5)
γ [°]	90	90
V [Å^3]	4292.9(3)	1045.47(11)
Z	8	2
D_{calcd} [g cm^{-3}]	1.640	1.683
$F(000)$	2112	528
μ [mm^{-1}]	3.801	3.902
Crystal size [mm^3]	0.32 × 0.31 × 0.31	0.24 × 0.19 × 0.13
Rflns collected	92 971	14 759
Independent rflns (R_{int})	9294 (0.0782)	2137 (0.0915)
Data/restraints/parameters	9294/0/541	2137/0/136
GOF on F^2	1.025	0.965
R_1, wR_2 [$I > 2\sigma(I)$]	0.0598, 0.1343	0.0293, 0.0660
R_1, wR_2 (all data)	0.1048, 0.1562	0.0415, 0.0696
Largest diff. peak and hole [e Å^{-3}]	0.553, −1.016	0.347, −0.570

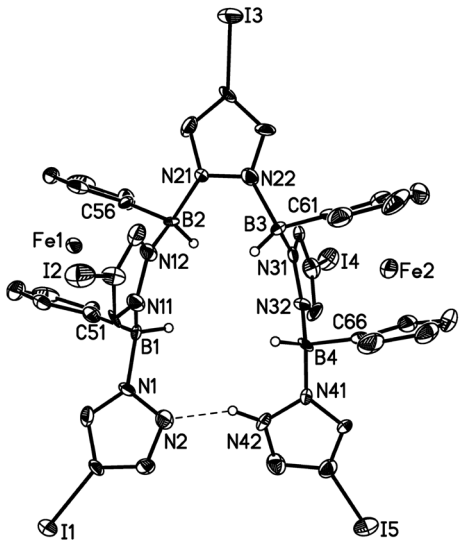

Fig. 3 Molecular structure of **3f***·3C_6H_6 in the solid state. Hydrogen atoms (except on boron and N(42)) and the C_6H_6 molecules have been omitted for clarity; displacement ellipsoids are drawn at the 50% probability level. The bond lengths and bond angles are not given due to poor crystallographic data which lead to large error margins. The H atom at N(42) was found in the difference Fourier map, but it could not be isotropically refined.

only. A third ring acts as a linker between the organometallic units, whereas the remaining two heterocyclic rings are terminal substituents. A proton residing on the nitrogen atom N(42) forms a hydrogen bond with the nitrogen atom N(2) to give a HB_4N_{10} macrocycle.

Compounds **3a**, [**4a**]Br and [**4b**]Br have also been characterised by X-ray crystallography (Fig. 4 and 5). Compounds **3a** and [**4b**]$^+$ possess no symmetry element in the crystal lattice; the solid-state structure of the cation [**4a**]$^+$ features a mirror plane containing the pyrazolyl ring pz(N(1)). All three molecules exhibit the aimed-for paddle-wheel structure with angles between the three core planes [B(1)N(1)N(2)B(2), B(1)N(11)-N(12)B(2) and B(1)C(21)C(22)B(2) (**3a**) or B(1)N(11A)N(12A)B(2) ([**4a**]Br) or B(1)N(21)N(22)B(2) ([**4b**]Br)] close to 120°.[30] The same is true for the angles between the corresponding planes in Li[**2a**] (Fig. 2).[19] In the cases of the two cationic B–N triptycenes, we observe kinks along certain N–N bonds resulting in dihedral angles between the pyrazolyl blades that can be as small as pz(N(11))//pz(N(11A)) = 100.6(1)° ([**4a**]Br) or as large as pz(N(1))//pz(N(21)) = 138.7(2)° ([**4b**]Br).

The average B–N bond lengths decrease continuously upon going from Li[**2a**] (1.605 Å) to **3a** (1.579 Å) to [**4b**]Br (1.562 Å). For [**4a**]Br, a comparison of the average B–N bond lengths about B(1) (1.570 Å) and B(2) (1.546 Å) indicates considerable steric repulsion between the *p*-BrC_6H_4 substituent and the bridging pyrazolide moieties. A related effect is obvious in the case of 9-phenyltriptycene, which shows longer endocyclic C–C bonds about the phenylated bridgehead carbon atom (average value = 1.554 Å) than about the unsubstituted bridgehead atom (average value = 1.513 Å).[31]

Similar to the B–N bonds, the intramolecular B···B distances contract along the series Li[**2a**] (2.734(6) Å) → **3a** (2.707(5) Å) → [**4a**]Br (2.676(6) Å)/[**4b**]Br (2.702(5) Å). Even shorter through-space distances are found between the two bridgehead carbon atoms in 9-phenyltriptycene (2.630 Å)[31] and in pristine triptycene (2.604 Å).[32]

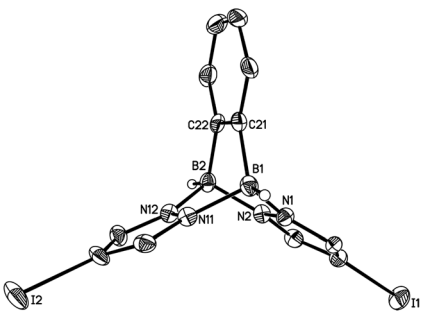

Fig. 4 Molecular structure of **3a** in the solid state. Hydrogen atoms except on boron have been omitted for clarity; displacement ellipsoids are drawn at the 50% probability level. Selected bond lengths (Å), atom···atom distance (Å), bond angles (°) and dihedral angles (°): B(1)–N(1) 1.575(4), B(1)–N(11) 1.588(4), B(1)–C(21) 1.611(5), B(2)–N(2) 1.574(4), B(2)–N(12) 1.579(4), B(2)–C(22) 1.604(5), B(1)···B(2) 2.707(5); N(1)–B(1)–N(11) 101.5(2), N(1)–B(1)–C(21) 105.7(3), N(11)–B(1)–C(21) 104.0(2), N(2)–B(2)–N(12) 100.9(2), N(2)–B(2)–C(22) 105.8(3), N(12)–B(2)–C(22) 104.4(3); N(1)B(1)N(11)//N(2)B(2)N(12) 84.1(3), N(1)B(1)N(11)//N(1)N(2)-N(11)N(12) 47.7(2), N(2)B(2)N(12)//N(1)N(2)N(11)N(12) 48.2(3), B(1)N(1)-N(2)B(2)//B(1)N(11)N(12)B(2) 117.3(1), B(1)N(1)N(2)B(2)//B(1)C(21)C(22)B(2) 122.4(2), B(1)N(11)N(12)B(2)//B(1)C(21)C(22)B(2) 120.3(2), pz(N(1))//pz-(N(11)) 123.0(1), pz(N(1))//C_6H_4 122.5(1), pz(N(11))//C_6H_4 114.4(1); pz(N(X)) = pyrazolyl ring containing N(X).

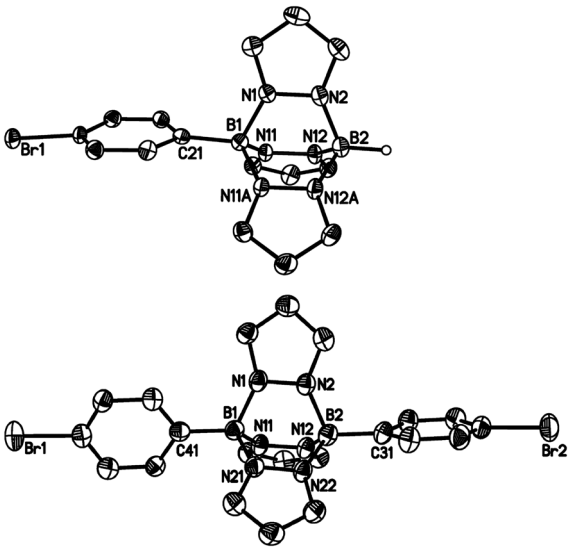

Fig. 5 Molecular structures of [**4a**]Br·CH_2Cl_2 (top) and [**4b**]Br (bottom) in the solid state. Hydrogen atoms except on boron, the bromide counterions and the solvent molecule have been omitted for clarity; displacement ellipsoids are drawn at the 50% probability level. Selected bond lengths (Å), atom···atom distances (Å), bond angles (°) and dihedral angles (°): [**4a**]Br: B(1)–N(1) 1.561(5), B(1)–N(11) 1.574(3), B(1)–C(21) 1.582(5), B(2)–N(2) 1.541(6), B(2)–N(12) 1.549(3), B(1)···B(2) 2.676(6); N(1)–B(1)–N(11) 104.4(2), N(11)–B(1)–N(11A) 101.3(3), N(2)–B(2)–N(12) 104.8(2), N(12)–B(2)–N(12A) 102.7(3); B(1)N(1)N(2)B(2)//B(1)N(11)N(12)B(2) 121.3(1), B(1)N(11)N(12)B(2)//B(1)N(11A)N(12A)B(2) 117.5(1), pz(N(1))//pz(N(11)) 129.7(1), pz(N(11))//pz(N(11A)) 100.6(1); symmetry transformation used to generate equivalent atoms: A: *x*, –*y* + 3/2, *z*. [**4b**]Br: B(1)–N(1) 1.561(5), B(1)–N(11) 1.558(5), B(1)–N(21) 1.563(4), B(1)–C(41) 1.589(5), B(2)–N(2) 1.561(5), B(2)–N(12) 1.575(5), B(2)–N(22) 1.556(5), B(2)–C(31) 1.590(5), B(1)···B(2) 2.702(5); N(1)–B(1)–N(11) 102.8(3), N(1)–B(1)–N(21) 103.9(3), N(11)–B(1)–N(21) 103.2(3), N(2)–B(2)–N(12) 102.6(3), N(2)–B(2)–N(22) 104.5(3), N(12)–B(2)–N(22) 102.5(3); B(1)N(1)N(2)B(2)//B(1)N(11)N(12)B(2) 119.0(2), B(1)N(1)N(2)B(2)//B(1)N(21)N(22)B(2) 121.6(2), B(1)N(11)N(12)B(2)//B(1)N(21)N(22)B(2) 119.4(2), pz(N(1))//pz(N(11)) 105.6(1), pz(N(1))//pz(N(21)) 138.7(2), pz(N(11))//pz(N(21)) 115.5(1); pz(N(X)) = pyrazolyl ring containing N(X).

Investigations into the relative cage stabilities of B–N triptycenes

Hydroboration reactions of alkenes and alkynes require three-coordinate hydroborane species.[33] If borane adducts are employed (*e.g.*, BH_3·SMe_2), the donor has to come off first in a preceding association–dissociation equilibrium step, before the B–H bond is able to add across a C=C-double or a C≡C-triple bond. A comparison of the reactivities of Li[**2a**] (Fig. 2), **3b** and [**4a**]Br toward the hydroboration of *t*BuC≡CH therefore provides useful first insight into the relative stabilities of the individual B–N cage bonds. Upon treatment with excess *t*BuC≡CH in THF at 60 °C, Li[**2a**] adds two equivalents of the alkyne to give Li[*t*BuC(H)=(H)CB(μ-pz^{TMS})-(μ-*o*-C_6H_4)$_2$BC(H)=(H)C*t*Bu] (Hpz^{TMS} = 4-(trimethylsilyl)pyrazole).[19] Under the same conditions, neither **3b** nor [**4a**]Br undergoes a hydroboration reaction, but can be recovered in essentially quantitative yield; this result remains valid if the temperature is increased to 80 °C.

In a second series of experiments, we investigated the sensitivity of B–N triptycenes toward air and moisture. While the B–H bonds of free 9,10-dihydro-9,10-diboraanthracene are extremely prone to hydrolysis,[34] it takes several hours until the ^{1}H NMR spectrum of compound Li[**2a**] in non-dried d_8-THF shows significant signs of decomposition.[19] In the cases of **3b**, [**4a**]Br and [**4b**]Br, even quick aqueous workup is possible; **3b** can also be purified by column chromatography under ambient conditions (silica gel, non-dried solvents). Further detailed protonolysis reactions were carried out in non-dried CD_3OD at room temperature and were monitored by NMR spectroscopy (plots of the spectra are included in the ESI,† together with the spectra of selected authentic samples of proposed decomposition products). ^{1}H NMR spectra recorded on solutions of compound **3b** approximately 10 min after sample preparation already contained resonances assignable to degradation products. After 2 h, about 10% of the initial amount of **3b** was left and after 2 d, the sample consisted exclusively of Dpz^{TMS} and *o*-C_6H_4(B$(OCD_3)_2)_2$ (**9**) in a stoichiometric ratio of 2 : 1 (Scheme 2; for simplicity reasons, we have drawn the

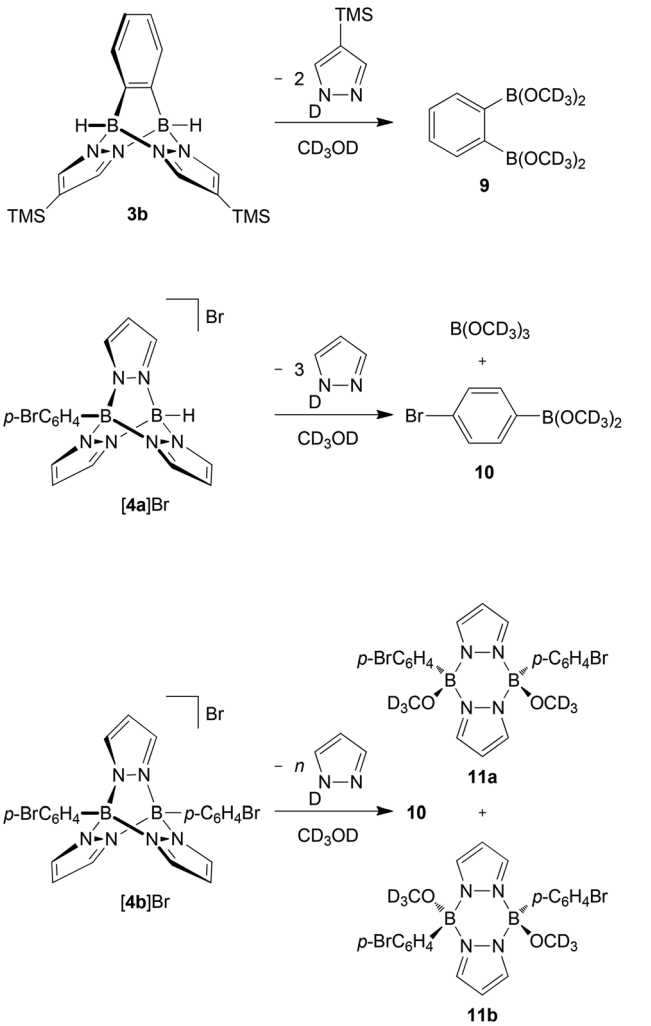

Scheme 2 Degradation reactions of **3b**, [**4a**]Br and [**4b**]Br in non-dried CD_3OD.

decomposition products as CD_3OD esters, even though the corresponding boronic acids or mixed acid/ester species may well be present, too). Under the same measurement conditions, about 55% of [**4a**]Br was still present in the sample after 2 h. Two days later, however, the proton NMR spectrum showed only the resonances of free pyrazole, together with a broad multiplet at 7.48–7.52 ppm. The $^{11}B\{^1H\}$ NMR spectrum contained resonances at 28.3 ppm and 18.6 ppm with an integral ratio of 1 : 1.4. The first value is characteristic of boron nuclei surrounded by one carbon and two oxygen atoms (*cf.* $C_6H_5B(OCH_3)_2$: $\delta(^{11}B)$ = 28.6[29]), whereas the second signal corresponds to $B(OCD_3)_3$ (*cf.* $B(OCH_3)_3$: $\delta(^{11}B)$ = 18.3; in CH_3OH[29,35]). These data thus indicate that the cage of [**4a**]Br has completely been broken down to pyrazole, the *p*-bromophenylboronic acid methyl ester **10** (resulting from the substituted bridgehead boron atom) and $B(OCD_3)_3$ (resulting from the unsubstituted bridgehead boron atom; Scheme 2).

The diphenylated derivative [**4b**]Br turned out to be more stable towards CD_3OD than **3b** and [**4a**]Br. After 76 d, ^1H NMR spectroscopy indicated the formation of four major products: (i) free pyrazole, (ii) **10** and (iii) two more species still consisting of both pyrazolide and *p*-BrC_6H_4 units. From the NMR tube, we were able to isolate the *syn* and *anti* pyrazaboles **11a**[36] and **11b** in a single-crystal form (Fig. 6). Since the molecular structures of **11a** and **11b** are consistent with the proton resonance patterns of the two incompletely degraded species, we conclude that pyrazaboles are comparatively long-lived intermediates of the protonolysis pathway of [**4b**]Br.[36] In line with that, the ^{11}B NMR spectrum of [**4b**]Br in CD_3OD after 76 d exhibited a resonance not only at 28.6 ppm (**10**), but also at 3.7 ppm (*cf.* $(C_6H_5)(CH_3O)B(\mu\text{-pz})_2B(OCH_3)(C_6H_5)$: $\delta(^{11}B)$ = 3.5;[37] in $CDCl_3$).

Compound **11a** crystallises from CD_3OD with two crystallographically independent molecules in the asymmetric unit (**11a^A**, **11a^B**). Since all key structural parameters of **11a^A** and **11a^B** are the same within the error margins, only the data for **11a^A** are compiled in Fig. 6. The pyrazabole core of **11a^A** adopts a boat conformation such that the two phenyl rings become almost coplanar. The two boron atoms are 3.115(7) Å apart from each other and the distance between the phenyl-ring centroids amounts to 3.808 Å. The C_i-symmetric molecule **11b** features a central B_2N_4 ring in a shallow chair conformation and a crystallographically imposed dihedral angle between the two pyrazolide rings of 0°.

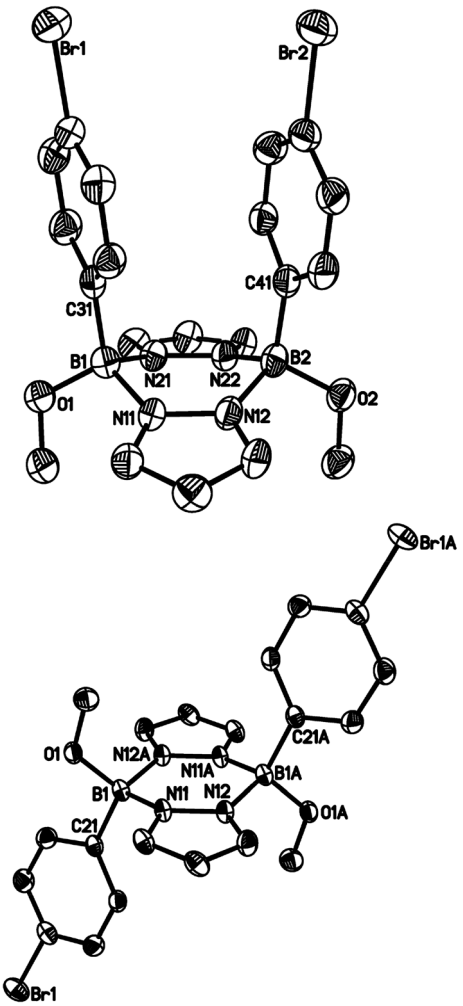

Fig. 6 Molecular structures of **11a^A** (top) and **11b** (bottom) in the solid state. Hydrogen atoms have been omitted for clarity; displacement ellipsoids are drawn at the 50% probability level. Selected bond lengths (Å), atom···atom distances (Å), bond angles (°) and dihedral angles (°): **11a^A**: B(1)–O(1) 1.415(6), B(1)–N(11) 1.577(6), B(1)–N(21) 1.587(6), B(1)–C(31) 1.602(7), B(2)–O(2) 1.442(6), B(2)–N(12) 1.600(6), B(2)–N(22) 1.578(6), B(2)–C(41) 1.589(7), B(1)···B(2) 3.115(7), COG(Ar(C(31)))···COG(Ar(C(41))) 3.808; N(11)–B(1)–N(21) 103.7(4), N(12)–B(2)–N(22) 103.0(3); N(11)B(1)N(21)//N(12)B(2)N(22) 54.6(3), N(11)B(1)N(21)//N(11)N(12)N(21)N(22) 27.5(3), N(12)B(2)N(22)//N(11)N(12)N(21)N(22) 27.1(3), B(1)N(11)N(12)B(2)//B(1)N(21)N(22)B(2) 140.2(2), pz(N(11))//pz(N(21)) 154.1(1), Ar(C(31))//Ar(C(41)) 9.3(1); Ar(C(X)) = aryl ring containing C(X); COG(Ar(C(X))) = centroid of the aryl ring containing C(X). **11b**: B(1)–O(1) 1.428(3), B(1)–N(11) 1.568(3), B(1)–N(12A) 1.597(3), B(1)–C(21) 1.615(3), B(1)···B(1A) 3.266(5); N(11)–B(1)–N(12A) 104.9(2); N(11)B(1)N(12A)//N(11)N(12)N(11A)N(12A) 14.3(3), pz(N(11))//pz(N(11A)) 0; pz(N(X)) = pyrazolyl ring containing N(X). Symmetry transformation used to generate equivalent atoms: A: $-x$, $-y+1$, $-z+1$.

C–C coupling reactions on a B–N triptycene platform

Using compound [**4c**]Br, we compared the relative performance of Sonogashira-[38] *versus* Stille-type[39,40] C–C-coupling protocols for the introduction of alkynyl substituents into B–N triptycene scaffolds (Scheme 3). The room-temperature reaction between [**4c**]Br and *t*BuC≡CH in dry NEt_3 using $PdCl_2(dppf)\cdot CH_2Cl_2$/CuI as the catalyst system afforded [**4e**]Br in approximately 45% yield after 7 d. (*Note*: It took 7 d until the last traces of the starting material had vanished in the ^1H NMR spectrum of the reaction mixture.) For reasons of simplicity, we still refer to the reaction product as [**4e**]Br (instead of [**4e**]X (X = Cl, Br or I)), even though some of the bromide counterions will likely be exchanged against chloride and/or iodide ions under the conditions applied. The ill-defined nature of the counterion in the reaction product is one shortcoming of the Sonogashira protocol, because it affects the calculation of precise stoichiometries as well as the determination of accurate yields. Another setback arises from the waste salt, $[HNEt_3]X$,

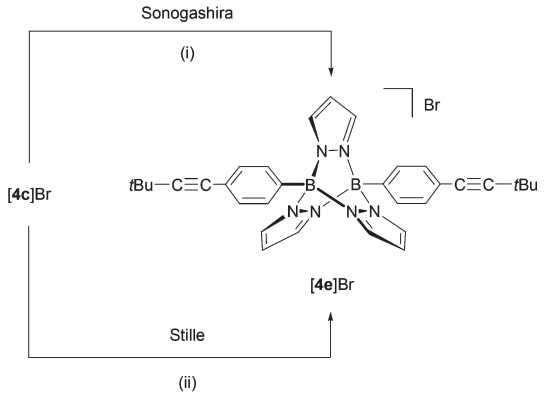

Scheme 3 Derivatisation of [**4c**]Br through Sonogashira-type and Stille-type coupling reactions. Reaction conditions: (i) +2 *t*BuC≡CH, +$PdCl_2$(dppf)·CH_2Cl_2/CuI (10 mol%), NEt_3, rt, 7 d. (ii) +2 $nBu_3SnC{\equiv}CtBu$, +$Pd(PtBu_3)_2$ (15 mol %), CH_3CN–toluene, rt, 24 h.

which is difficult to separate completely from the target compound. These problems did not occur upon application of the Stille protocol ($nBu_3SnC{\equiv}CtBu$, CH_3CN–toluene, 15 mol% $Pd(PtBu_3)_2$), which gave comparable yields of [**4e**]Br as the Sonogashira reaction and required a reaction time of only 24 h at room temperature.

The B–N cage of [**4e**]Br revealed similar NMR characteristics to the other symmetrically substituted $[\mathbf{4}]^+$-type compounds. A singlet at 1.38 ppm in the ^{1}H NMR spectrum is to be assigned to the *tert*-butyl substituents. The ^{13}C NMR resonances of the alkynyl–carbon atoms appear at 101.7 ppm and 78.4 ppm.

Synthesis and characterisation of B–N-analogues of pentiptycenes

The key to success for the synthesis of **3**-type B–N triptycenes was the availability of the lithium 1,2-bisborate Li_2[**7**] (Scheme 1). Recently, we have also prepared the lithium 1,2,4,5-tetrakisborate Li_4[**13**],[41] which can consequently be employed for the synthesis of B–N pentiptycenes **14a–14d** (Scheme 4). The general synthesis protocol for **14a–14d** was essentially the same as that previously described in the cases of **3a–3e**. We note, however, a markedly reduced solubility of some B–N pentiptycenes as compared to the B–N triptycenes (the same is true for the all-carbon frameworks).[4] For example, the CF_3 derivative **14a** was obtained from toluene in an analytically pure, single-crystalline form; however, the crystals did not re-dissolve in any common inert solvent. Compound **14a** was therefore characterised only by elemental analysis and X-ray crystallography (Fig. 7, top). The introduction of $SiMe_3$

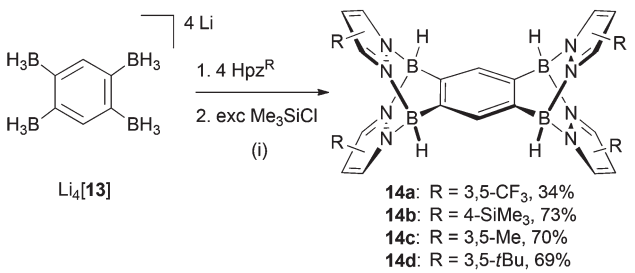

Scheme 4 Synthesis of the B–N pentiptycenes **14a–14d**. General reaction conditions: (i) THF or toluene, rt or 80 °C, between 1 d and 7 d.

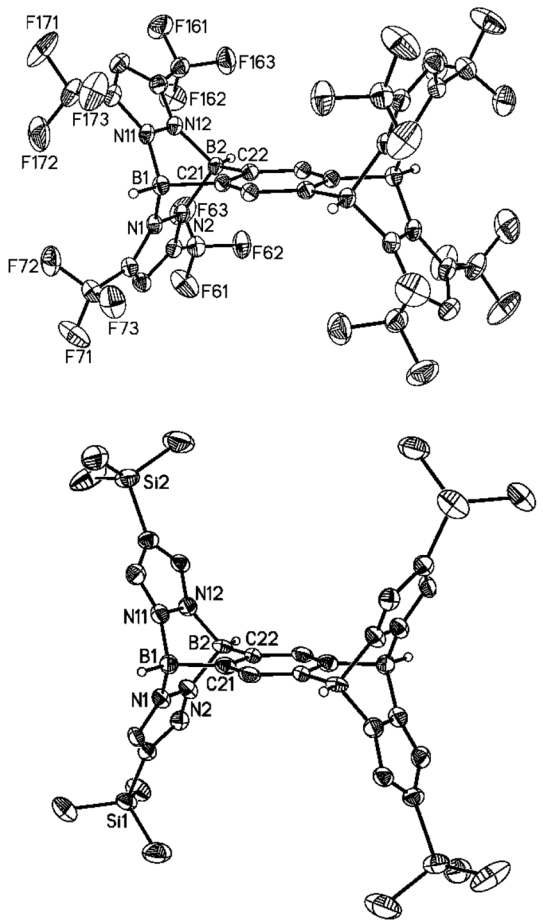

Fig. 7 Molecular structures of **14a**·$3C_7H_8$ (top) and **14b**·$2CH_2Cl_2$ (bottom) in the solid state. Hydrogen atoms except on boron and the solvent molecules have been omitted for clarity; displacement ellipsoids are drawn at the 50% probability level. Selected bond lengths (Å), atom···atom distances (Å), bond angles (°) and dihedral angles (°): **14a**: B(1)–N(1) 1.601(2), B(1)–N(11) 1.595(3), B(1)–C(21) 1.597(2), B(2)–N(2) 1.601(2), B(2)–N(12) 1.601(2), B(2)–C(22) 1.595(3), B(1)···B(2) 2.712(3); N(1)–B(1)–N(11) 99.7(1), N(1)–B(1)–C(21) 105.1(1), N(11)–B(1)–C(21) 106.1(1), N(2)–B(2)–N(12) 99.5(1), N(2)–B(2)–C(22) 105.5(1), N(12)–B(2)–C(22) 106.0(1); N(1)B(1)N(11)//N(2)B(2)N(12) 82.4(1), N(1)B(1)N(11)//N(1)-N(2)N(11)N(12) 48.6(1), N(2)B(2)N(12)//N(1)N(2)N(11)N(12) 49.0(1), B(1)-N(1)N(2)B(2)//B(1)N(11)N(12)B(2) 115.1(1), B(1)N(1)N(2)B(2)//B(1)C(21)C(22)-B(2) 121.92(7), B(1)N(11)N(12)B(2)//B(1)C(21)C(22)B(2) 123.00(9), pz(N(1))// pz(N(11)) 117.77(8), pz(N(1))//C_6H_2 117.15(6), pz(N(11))//C_6H_2 125.07(8). **14b**: B(1)–N(1) 1.574(9), B(1)–N(11) 1.590(8), B(1)–C(21) 1.597(9), B(2)–N(2) 1.593(7), B(2)–N(12) 1.578(8), B(2)–C(22) 1.597(9), B(1)···B(2) 2.701(1); N(1)–B(1)–N(11) 101.7(5), N(1)–B(1)–C(21) 105.9(5), N(11)–B(1)–C(21) 105.3(4), N(2)–B(2)–N(12) 100.9(5), N(2)–B(2)–C(22) 105.3(4), N(12)–B(2)–C(22) 104.1(5); N(1)B(1)N(11)//N(2)B(2)N(12) 84.0(6), N(1)B(1)N(11)//N(1)N(2)N(11)N(12) 48.7(5), N(2)B(2)N(12)//N(1)N(2)N(11)N(12) 47.3(4), B(1)-N(1)N(2)B(2)//B(1)N(11)N(12)B(2) 117.3(3), B(1)N(1)N(2)B(2)//B(1)C(21)C(22)-B(2) 122.0(3), B(1)N(11)N(12)B(2)//B(1)C(21)C(22)B(2) 120.7(3), pz(N(1))//-pz(N(11)) 127.2(3), pz(N(1))//C_6H_2 120.4(3), pz(N(11))//C_6H_2 112.4(3); pz(N(X)) = pyrazolyl ring containing N(X).

substituents in the 4-position of the pyrazolyl rings leads to good solubility of **14b** in C_6H_6, toluene, $CHCl_3$, CH_2Cl_2 or THF; NMR spectra were recorded in C_6D_6. The ^{1}H NMR spectrum of **14b** reveals a singlet at 8.66 ppm for the two protons on the central six-membered ring, another singlet at 7.35 ppm for the eight magnetically equivalent hydrogen atoms on the pyrazolyl fragments and one resonance at −0.08 ppm for the $SiMe_3$ groups (36 H). The $^{11}B\{^1H\}$ NMR spectrum features one broad signal at −2.7 ppm (*cf.* **3b**: −3.2 ppm). The molecular structure of **14b** was finally confirmed also by X-ray crystallography (Fig. 7, bottom). The NMR spectra of the derivatives **14c** and **14d** ($CDCl_3$) show no peculiarities compared to those of **14b**; all corresponding data are compiled in the ESI.†

Both compounds, **14a** and **14b**, are C_i-symmetric in the solid state. All key metrical parameters of pentiptycene **14a** are similar to those of its triptycene analogue **3e** and the same applies to the bond lengths and angles of **14a** compared to **14b**. In the crystal lattice of **14a**·$3C_7H_8$, the void spaces between the pyrazolyl rings pz(N(1)) and pz(N(11)) as well as pz(N(1)) and pz(N(11A)) are occupied by toluene molecules. In the case of **14b**·$2CH_2Cl_2$, only the compartments above and below the central six-membered ring are hosting solvent molecules.

Conclusion

The concept of B–N/C–C isosterism was applied for the development of a complete series of B–N analogues of triptycene, *i.e.* $[HB(\mu\text{-}pz^R)(\mu\text{-}o\text{-}C_6H_4)_2BH]^-$ ($[\mathbf{2}]^-$), $HB(\mu\text{-}pz^R)_2(\mu\text{-}o\text{-}C_6H_4)BH$ (**3**) and $[RB(\mu\text{-}pz^R)_3BR']^+$ ($[\mathbf{4}]^+$). Instead of employing highly reactive benzyne intermediates, as they are required to prepare all-carbon triptycenes, the synthesis of the B–N congeners relies on the facile formation of B–N adduct bonds. We have also shown that the general design strategy can be extended to the preparation of B–N analogues of pentiptycene. Most of the compounds are sufficiently stable towards air and moisture to allow for a quick aqueous workup. As a proof-of-principle, we have also shown that the molecular framework of **4**-type compounds is compatible with further derivatisation through Stille-type C–C-coupling protocols. Thus, B–N iptycenes are highly promising building blocks for the facile assembly of rigid supramolecular frameworks with selectable overall charges.

Experimental methods

Unless otherwise specified, all reactions were carried out in carefully dried solvents under dry nitrogen or argon using Schlenk or glove-box techniques. *n*-Pentane, *n*-hexane, cyclohexane, C_6H_6, C_6D_6, toluene, THF, d_8-THF and Et_2O were dried over Na/benzophenone; NEt_3, CH_3CN, CD_3CN, $CHCl_3$, $CDCl_3$, CH_2Cl_2 and Me_3SiCl were dried over CaH_2 and freshly distilled prior to use. Column chromatography was performed using silica gel 60 (Macherey-Nagel). NMR spectra were recorded at rt with Bruker AM 250, DPX 250, Avance II 300, Avance 400 and Avance III HD 500 spectrometers. Chemical shifts are referenced to (residual) solvent signals ($^1H/^{13}C\{^1H\}$; C_6D_6: 7.16/128.06; d_8-THF: 1.72/25.31; CD_3CN: 1.94/1.32; $CDCl_3$: 7.26/77.16; CD_3OD: 3.31/49.00) or external $BF_3{\cdot}OEt_2$ (^{11}B,$^{11}B\{^1H\}$) and $Si(CH_3)_4$ (^{29}Si INEPT). Abbreviations: s = singlet, d = doublet, tr = triplet, vtr = virtual triplet, q = quartet, m = multiplet, br = broad, n.o. = signal not observed; n.r. = multiplet expected in the ^{1}H NMR spectrum but not resolved. Combustion analyses were performed by the Microanalytical Laboratory of the Goethe University Frankfurt; HRMS measurements were performed on a MALDI LTQ Orbitrap spectrometer (Thermo Scientific). The compounds $Li_2[7]{\cdot}OEt_2$,[23] $Li_2[1,1'\text{-}fc(BH_3)_2]{\cdot}(OEt_2)_{0.25}$,[25] $K[HBpz_3]$,[42] $K[p\text{-}BrC_6H_4Bpz_3]$,[43] $p\text{-}BrC_6H_4BBr_2$,[44] 4-iodopyrazole,[45] $nBu_3SnC{\equiv}CtBu$,[46] 4-(trimethylsilyl)pyrazole,[47] and 3,5-di(*tert*-butyl)pyrazole[48] are literature known; the amount of OEt_2 present in the samples of $Li_2[1,1'\text{-}fc(BH_3)_2]{\cdot}(OEt_2)_{0.25}$ after prolonged storage in a screw-capped vial in the glove-box was determined by ^{1}H NMR spectroscopy.

Synthesis of 3a

A Schlenk flask was charged with $Li_2[7]{\cdot}OEt_2$ (50 mg, 0.26 mmol) and 4-iodopyrazole (101 mg, 0.521 mmol). Et_2O (10 mL) was added at rt with stirring, whereupon vigorous gas evolution (H_2) was observed, which lasted for approximately 2 min. After 30 min, neat Me_3SiCl (0.1 mL, 0.08 g, 0.8 mmol) was added to the light yellow solution to give a white suspension. Stirring was continued for 12 h, the formed LiCl was removed by filtration and the filtrate was evaporated under vacuum to yield a colourless solid. Single crystals were grown by slow evaporation of a solution of **3a** in Et_2O. Yield: 89 mg, 70%. ^{1}H NMR (300.0 MHz, C_6D_6): δ = 7.85–7.79 (2 H, m, H-3,6), 7.30–7.24 (2 H, m, H-4,5), 6.84 (4 H, s, pzH-3,5), 4.25* (2 H, br, BH); $^{13}C\{^1H\}$ NMR (75.4 MHz, C_6D_6): δ = 138.5 (pzC-3,5), 130.3 (C-3,6), 126.6 (C-4,5), 55.7 (pzC-4), n.o. (CB); $^{11}B\{^1H\}$ NMR (96.3 MHz, C_6D_6): δ = −3.7 ($h_{1/2}$ = 240 Hz); HRMS (MALDI-TOF): m/z = 486.92435 ($[M + H]^+$, calcd 486.92537). *This signal sharpens upon ^{11}B decoupling.

Synthesis of 3b

A Schlenk flask was charged with $Li_2[7]{\cdot}OEt_2$ (0.1 g, 0.5 mmol) and 4-(trimethylsilyl)pyrazole (0.15 g, 1.1 mmol). Et_2O (20 mL) was added at rt with stirring, whereupon vigorous gas evolution (H_2) was observed, which lasted for approximately 2 min. After 30 min, neat Me_3SiCl (0.20 mL, 0.17 g, 1.6 mmol) was added to the pale yellow solution to give a white suspension. Stirring was continued for 12 h, the formed LiCl was removed by filtration and the filtrate was evaporated under vacuum to yield a colourless solid. The solid was suspended in *n*-hexane (20 mL) and quenched with saturated brine (10 mL). The two liquid phases were separated from each other and the aqueous phase was extracted with *n*-hexane (20 mL). The combined organic phases were quickly extracted with H_2O (20 mL), dried over anhydrous $MgSO_4$, filtered, and the filtrate was evaporated to dryness under vacuum. The crude product was further

purified by short column chromatography (silica gel, ethyl acetate, R_f = 0.86). Yield: 103 mg (52%). (Found: C, 57.22; H, 7.76; N, 14.52. Calc. for $C_{18}H_{28}B_2N_4Si_2$ [378.24]: C, 57.16; H, 7.46; N, 14.81%.) ^{1}H NMR (400.1 MHz, C_6D_6): δ = 8.04–8.00 (2 H, m, H-3,6), 7.35 (4 H, s, pzH-3,5), 7.32–7.28 (2 H, m, H-4,5), 4.84* (2 H, br, BH), −0.07 (18 H, s, $SiMe_3$); $^{13}C\{^1H\}$ NMR (100.6 MHz, C_6D_6): δ = 138.2 (pzC-3,5), 130.3 (C-3,6), 126.4 (C-4,5), 114.5 (pz-C4), −0.6 ($SiMe_3$), n.o. (CB); $^{11}B\{^1H\}$ NMR (128.4 MHz, C_6D_6): δ = −3.2 ($h_{1/2}$ = 300 Hz); ^{29}Si INEPT NMR (79.5 MHz, C_6D_6): δ = −10.6. *This signal sharpens upon ^{11}B decoupling.

Synthesis of 3f

A Schlenk flask was charged with $Li_2[1,1'\text{-fc}(BH_3)_2]\cdot(OEt_2)_{0.25}$ (50 mg, 0.20 mmol) and 4-iodopyrazole (81 mg, 0.42 mmol). Et_2O (10 mL) was added at rt with stirring, whereupon vigorous gas evolution (H_2) was observed, which lasted for approximately 2 min. After 30 min, neat Me_3SiCl (0.1 mL, 0.08 g, 0.8 mmol) was added to the yellow solution to give a white suspension. Stirring was continued for 12 h, the formed LiCl was removed by filtration and the filtrate was evaporated under vacuum. The remaining orange solid was dissolved in Et_2O and the solution was stored at −30 °C to grow single crystals of **3f**·OEt_2. Yield: 104 mg, 76%. ^{1}H NMR (300.0 MHz, C_6D_6): δ = 7.03 (4 H, s, pzH-3,5), 4.12 (4 H, vtr, $J_{H,H}$ = 1.7 Hz, C_5H_4), 3.22 (4 H, vtr, $J_{H,H}$ = 1.7 Hz, C_5H_4), n.o. (BH); $^{13}C\{^1H\}$ NMR (75.4 MHz, C_6D_6): δ = 140.5 (pzC-3,5), 70.9 (C_5H_4), 70.3 (C_5H_4), 56.3 (pzC-4), n.o. (CB); $^{11}B\{^1H\}$ NMR (96.3 MHz, C_6D_6): δ = −3.5 ($h_{1/2}$ = 240 Hz); MS (MALDI-TOF): m/z 593.8 ($[M]^+$, 100%); HRMS (MALDI-TOF): m/z = 593.88323 ($[M]^+$, calcd 593.88379).

Synthesis of [4a]Br

A solution of p-$BrC_6H_4BBr_2$ (194 mg, 0.594 mmol) in toluene (15 mL) was added dropwise with stirring at rt to a solution of $K[HBpz_3]$ (150 mg, 0.595 mmol) in CH_3CN–toluene (1 : 1, 20 mL). The resulting mixture was stirred for 24 h at rt. All insolubles were collected on a frit and quickly washed with H_2O (3 mL) to remove KBr. The crude product was immediately after that washed with n-pentane (2 × 15 mL) and dried under vacuum. Single crystals were grown by slow evaporation of a solution of [**4a**]Br in CH_2Cl_2. Yield: 255 mg, 93%. ^{1}H NMR (500.2 MHz, CD_3CN): δ = 8.24 (3 H, d, $^3J_{H,H}$ = 2.5 Hz, pzH-3 or pzH-5), 8.02 (3 H, d, $^3J_{H,H}$ = 2.5 Hz, pzH-3 or pzH-5), 7.91 (2 H, d, $^3J_{H,H}$ = 8.5 Hz, ArH), 7.84 (2 H, d, $^3J_{H,H}$ = 8.5 Hz, ArH), 6.51 (3 H, vtr, pzH-4), 5.35–4.30 (1 H, br m, BH). $^{13}C\{^1H\}$ NMR (125.8 MHz, CD_3CN): 139.7 (pzC-3 or pzC-5), 139.2 (pzC-3 or pzC-5), 136.5 (ArC), 133.1 (ArC), 125.6 (CBr), 108.6 (pzC-4), n.o. (CB); $^{11}B\{^1H\}$ NMR (160.5 MHz, CD_3CN): δ = −0.5 ($h_{1/2}$ = 110 Hz, BC), −5.4 ($h_{1/2}$ = 100 Hz, BH); ^{11}B NMR (160.5 MHz, CD_3CN): δ = −0.5 (s, BC), −5.4 (d, $^1J_{B,H}$ = 128 Hz, BH); MS (ESI^+): m/z 379.2 ($[M - Br]^+$, 100%); HRMS (MALDI-TOF): m/z = 379.06527 ($[M - Br]^+$, calcd 379.06439).

Synthesis of [4b]Br

In a Schlenk vessel equipped with a Teflon Young's tab, p-$BrC_6H_4BBr_2$ (40 mg, 0.12 mmol) was dissolved in toluene (15 mL). Neat solid $K[p\text{-}BrC_6H_4Bpz_3]$ (50 mg, 0.12 mmol) was added, the tab was closed and the vessel was heated with stirring for 8 h at 120 °C. After cooling to rt, all insolubles were collected on a frit and washed with n-pentane (6 × 5 mL). The solid material was suspended in $CHCl_3$ (20 mL) and quenched with a saturated aqueous solution of $NaHCO_3$ (10 mL). The two liquid phases were separated from each other and the aqueous phase was extracted with $CHCl_3$ (20 mL). The combined organic phases were washed with H_2O (20 mL), dried over anhydrous $MgSO_4$, filtered and the filtrate was evaporated to dryness under vacuum. Single crystals were obtained as colourless blocks by slow evaporation of a solution of [**4b**]Br in $CHCl_3$. Yield: 60 mg, 80%. (Found: C, 40.35; H, 2.87; N, 13.42. Calc. for $C_{21}H_{17}B_2Br_3N_6$ [614.76]: C, 41.03; H, 2.79; N, 13.67%.) ^{1}H NMR (500.2 MHz, CD_3CN): δ = 8.08 (6 H, d, $^3J_{H,H}$ = 2.5 Hz, pzH-3,5), 7.94 (4 H, d, $^3J_{H,H}$ = 8.3 Hz, ArH), 7.87 (4 H, d, $^3J_{H,H}$ = 8.3 Hz, ArH), 6.52 (3 H, tr, $^3J_{H,H}$ = 2.5 Hz, pzH-4); $^{13}C\{^1H\}$ NMR (75.4 MHz, CD_3CN): δ = 139.8 (pzC-3,5), 136.6 (ArC), 133.2 (ArC), 108.6 (pzC-4), n.o. (CBr), n.o. (CB); $^{11}B\{^1H\}$ NMR (96.3 MHz, CD_3CN): δ = −0.5 ($h_{1/2}$ = 160 Hz); HRMS (MALDI-TOF): m/z = 535.00411 ($[M - Br]^+$, calcd 535.00416).

Synthesis of [4c]Br

In a Schlenk vessel equipped with a Teflon Young's tab, p-$IC_6H_4BBr_2$ (123 mg, 0.330 mmol) was dissolved in toluene (15 mL). Neat solid $K[p\text{-}IC_6H_4Bpz_3]$ (150 mg, 0.330 mmol) was added, the tab was closed and the vessel was heated with stirring for 6 h at 120 °C. After cooling to rt, all insolubles were collected on a frit, washed with H_2O (20 mL), n-pentane (6 × 5 mL) and dried under vacuum. Yield: 196 mg, 84%. ^{1}H NMR (300.0 MHz, CD_3CN): δ = 8.11–8.04 (10 H, m, ArH, pzH-3,5), 7.79 (4 H, d, $^3J_{H,H}$ = 8.1 Hz, ArH), 6.52 (3 H, tr, $^3J_{H,H}$ = 2.5 Hz, pzH-4); $^{13}C\{^1H\}$ NMR (125.8 MHz, CD_3CN): δ = 139.7 (pzC-3,5), 139.2 (ArC), 136.4 (ArC), 108.6 (pzC-4), 97.9* (CI), n.o. (CB); ^{11}B NMR (96.3 MHz, CD_3CN): δ = −0.9 ($h_{1/2}$ = 230 Hz); HRMS (MALDI-TOF): m/z = 628.97883 ($[M - Br]^+$, calcd 628.97847). *The position of this signal was confirmed by an HMBC experiment.

Synthesis of [4d]Br

In a Schlenk vessel equipped with a Teflon Young's tab, p-$Me_3SiC_6H_4BBr_2$ (172 mg, 0.538 mmol) was dissolved in toluene (15 mL). Neat solid $K[p\text{-}Me_3SiC_6H_4Bpz_3]$ (215 mg, 0.537 mmol) was added, the tab was closed and the vessel was heated with stirring for 6 h at 120 °C. After cooling to rt, all insolubles were collected on a frit, washed with n-pentane (6 × 5 mL), suspended in $CHCl_3$ (20 mL) and quenched with a saturated aqueous solution of $NaHCO_3$ (10 mL). The two liquid phases were separated from each other and the aqueous phase was extracted with $CHCl_3$ (20 mL). The combined organic phases were washed with H_2O (20 mL), dried over anhydrous $MgSO_4$, filtered and the filtrate was evaporated to dryness under vacuum. Single crystals were obtained as colourless blocks by slow evaporation of a solution of [**4d**]Br in $CHCl_3$. Yield: 259 mg, 80%. (Found: C, 54.29; H, 6.11; N, 13.86. Calc. for $C_{27}H_{35}B_2BrN_6Si_2$ [601.30]: C, 53.93; H, 5.87; N, 13.98%.) ^{1}H

NMR (400.1 MHz, $CDCl_3$): δ = 8.12 (6 H, d, $^3J_{H,H}$ = 2.5 Hz, pzH-3,5), 7.96 (4 H, d, $^3J_{H,H}$ = 8.0 Hz, ArH), 7.83 (4 H, d, $^3J_{H,H}$ = 8.0 Hz, ArH), 6.71 (3 H, tr, $^3J_{H,H}$ = 2.5 Hz, pzH-4), 0.36 (18 H, s, $SiMe_3$); $^{13}C\{^1H\}$ NMR (100.6 MHz, $CDCl_3$): δ = 144.4 (CSi), 138.8 (pzC-3,5), 134.6 (ArC), 132.5 (ArC), 108.9 (pzC-4), −1.1 ($SiMe_3$), n.o. (CB); ^{11}B NMR (128.4 MHz, $CDCl_3$): δ = 0.2 ($h_{1/2}$ = 400 Hz); ^{29}Si INEPT NMR (99.4 MHz, $CDCl_3$): δ = −3.3; MS (ESI^+): m/z 521.8 ($[M - Br]^+$, 100%).

Synthesis of [4e]Br

Method A: [**4c**]Br (50 mg, 0.071 mmol), $PdCl_2(dppf)\cdot CH_2Cl_2$ (6 mg, 0.007 mmol) and CuI (2 mg, 0.01 mmol) were suspended in NEt_3 (20 mL). *t*BuC≡CH (18 μL, 12 mg, 0.15 mmol) was added *via* a syringe and the solution was stirred for 7 d at rt. All volatiles were removed under reduced pressure. The remaining dark brown solid was washed with H_2O (20 mL), THF (20 mL), C_6H_6 (20 mL) and *n*-pentane (30 mL) to obtain a colourless solid, which was dried *in vacuo*. Yield: 21 mg, 48% (*note*: the product was still contaminated with small quantities of $[HNEt_3]X$ (X = Cl, Br or I); NMR spectroscopic control).

Method B: [**4c**]Br (20 mg, 0.028 mmol) and $Pd(PtBu_3)_2$ (2 mg, 0.004 mmol) were dissolved in CH_3CN (10 mL) and toluene (10 mL). Neat $nBu_3SnC{\equiv}CtBu$ (21 μL, 21 mg, 0.058 mmol) was added *via* a syringe and the clear yellow solution was stirred for 24 h at rt. All volatiles were removed under reduced pressure, the yellow solid residue was treated with C_6H_6 (10 mL) to give a yellow suspension, and the insoluble material was collected on a frit, washed with *n*-hexane (10 mL) and dried *in vacuo*. Yield: 8 mg, 46%.

^1H NMR (500.2 MHz, $CDCl_3$): δ = 8.11 (6 H, d, $^3J_{H,H}$ = 2.5 Hz, pzH-3,5), 7.95 (4 H, d, $^3J_{H,H}$ = 8.0 Hz, ArH), 7.72 (4 H, d, $^3J_{H,H}$ = 8.0 Hz, ArH), 6.66 (3 H, tr, $^3J_{H,H}$ = 2.5 Hz, pzH-4), 1.38 (18 H, s, CH_3); $^{13}C\{^1H\}$ NMR (125.8 MHz, $CDCl_3$): δ = 138.8 (pzC-3,5), 133.2 (ArC), 132.8 (ArC), 127.3* (*C*C≡C), 108.8 (pzC-4), 101.7* (*t*Bu*C*≡C), 78.4* (Ar*C*≡C), 31.1 (CH_3), 28.3 ($C(CH_3)$), n.o. (CB); ^{11}B NMR (96.3 MHz, CD_3CN): δ = 0.1 ($h_{1/2}$ = 500 Hz); HRMS (MALDI-TOF): m/z = 537.31069 ($[M - Br]^+$, calcd 537.31038). *The position of this signal was confirmed by an HMBC experiment.

Synthesis of 14a

A Schlenk flask was charged with Li_4[**13**]·3thf (50 mg, 0.13 mmol) and 3,5-bis(trifluoromethyl)pyrazole (0.11 g, 0.54 mmol). Toluene (20 mL) was added at rt with stirring, whereupon a gas (H_2) evolved. After 10 min, neat Me_3SiCl (0.1 mL, 0.08 g, 0.8 mmol) was added to the colourless suspension and stirring was continued for 4 d. All insolubles were collected on a frit (77 mg; 100% LiCl = 22 mg) and the filtrate was stored at 4 °C for 14 d to obtain block-shaped crystals of **14a**·$3C_7H_8$. Yield: 11 mg, 7%. The mother liquor was evaporated to dryness to give **14a** as a colourless solid; an elemental analysis revealed that, in contrast to the single crystals, the microcrystalline product no longer contained toluene. Yield: 34 mg, 27%. (Found: C, 33.55; H, 1.24; N, 12.01. Calc. for $C_{26}H_{10}B_4F_{24}N_8$ [933.62]: C, 33.45; H, 1.08; N, 12.00%.) Since **14a** did not re-dissolve in any common inert solvent, NMR data cannot be provided.

Synthesis of 14b

A Schlenk flask was charged with Li_4[**13**]·3thf (50 mg, 0.13 mmol) and 4-(trimethylsilyl)pyrazole (75 mg, 0.53 mmol). THF (20 mL) was added at rt and the resulting solution was stirred for 15 min; the reaction proceeds with evolution of H_2. Neat Me_3SiCl (0.1 mL, 0.08 g, 0.8 mmol) was added to the pale yellow solution and stirring was continued for 24 h. All volatiles were removed under vacuum. The yellow solid residue was extracted with toluene (20 mL). The extract was evaporated to dryness under vacuum to obtain **14b** as a colourless solid. Yield: 66 mg, 73%. Single crystals of **14b**·$2CH_2Cl_2$ were obtained in the form of colourless blocks by slow evaporation of a solution of **14b** in CH_2Cl_2.

^1H NMR (300.0 MHz, C_6D_6): δ = 8.66 (2 H, s, H-3,6), 7.35 (8 H, s, pzH-3,5), 4.96* (4 H, br, BH), −0.08 (36 H, s, $SiMe_3$); $^{13}C\{^1H\}$ NMR (75.4 MHz, C_6D_6): δ = 137.8 (pzC-3,5), 132.6 (C-3,6), 113.8 (pz-C4), −0.6 ($SiMe_3$), n.o. (CB); $^{11}B\{^1H\}$ NMR (96.3 MHz, C_6D_6): δ = −2.7 ($h_{1/2}$ = 900 Hz); ^{29}Si INEPT NMR (59.6 MHz, C_6D_6): δ = −10.8; HRMS (MALDI-TOF): m/z = 678.36164 ($[M]^+$, calcd 678.36253 ($C_{30}H_{50}B_4N_8Si_4$)). *This signal sharpens upon ^{11}B decoupling.

X-ray crystal structure determinations

Data for **11a**, **11b** and **12a** were collected on a STOE IPDS II two-circle diffractometer with graphite-monochromated MoK_α radiation (λ = 0.71073 Å) and corrected for absorption with an empirical absorption correction using the program *PLATON*.[49] Data for **3a**, **3c**, **3d**, **3e**, **3f**·OEt_2, **3f***·$3C_6H_6$, [**4a**]Br·CH_2Cl_2, [**4b**]Br, **14a**·$3C_7H_8$, and **14b**·$2CH_2Cl_2$ were collected on a STOE IPDS II two-circle diffractometer with a Genix Microfocus tube with mirror optics using MoK_α radiation (λ = 0.71073 Å) and were scaled using the frame scaling procedure in the *X-AREA* program system.[50] The structures were solved by direct methods using the program *SHELXS*[51] and refined against F^2 with full-matrix least-squares techniques using the program *SHELXL-97*.[51]

The H atoms bonded to B in **3a**, **3c**, **3e** and [**4a**]Br·CH_2Cl_2 were isotropically refined. The coordinates of the H atoms bonded to B in **3d** were refined. The crystal of **3a** was merohedrally twinned (twin law: −1 −1 0/0 1 0/0 0 −1) with a fractional contribution of 0.1971(7) for the minor domain. The crystal of **3f**·OEt_2 was very weakly diffracting. The displacement parameters of all B, N and C atoms were restrained to an isotropic behaviour. In **3f***·$3C_6H_6$, the displacement parameters of B2, B4 and the benzene-C atoms C71 to C76 as well as C91 to C96 were restrained to an isotropic behaviour. Bond lengths and angles in the benzene solvent molecules were restrained to be equal. One toluene molecule in **14a**·$3C_7H_8$ was disordered about a centre of inversion over two equally occupied positions; the H atoms bonded to B were isotropically refined. The crystal of **14b**·$2CH_2Cl_2$ was just weakly diffracting; the H atoms bonded to B were isotropically refined.

CCDC reference numbers: 985503 (**3a**), 985504 (**3c**), 985505 (**3d**), 985506 (**3e**), 985507 (**3f**·OEt_2), 985508 (**3f***·$3C_6H_6$), 985509 ([**4a**]Br·CH_2Cl_2), 985510 ([**4b**]Br), 985511 (**11a**), 985512 (**11b**), 985513 (**12a**), 985514 (**14a**·$3C_7H_8$) and 985515 (**14b**·$2CH_2Cl_2$).

Acknowledgements

This work has been supported by the Beilstein-Institut, Frankfurt/Main, Germany, within the research collaboration NanoBiC through a Ph.D. grant for Ö.S.

References

1 N. B. McKeown, P. M. Budd and D. Book, *Macromol. Rapid Commun.*, 2007, **28**, 995–1002.
2 H. Iwamura and K. Mislow, *Acc. Chem. Res.*, 1988, **21**, 175–182.
3 T. R. Kelly, *Acc. Chem. Res.*, 2001, **34**, 514–522.
4 C.-F. Chen and Y.-X. Ma, *Iptycenes Chemistry: From Synthesis to Applications*, Springer, Berlin, Heidelberg, 2013.
5 J. H. Chong and M. J. MacLachlan, *Chem. Soc. Rev.*, 2009, **38**, 3301–3315.
6 J. Liu, O. Shekhah, X. Stammer, H. K. Arslan, B. Liu, B. Schüpbach, A. Terfort and C. Wöll, *Materials*, 2012, **5**, 1581–1592.
7 T. M. Swager, *Acc. Chem. Res.*, 2008, **41**, 1181–1189.
8 C.-F. Chen, *Chem. Commun.*, 2011, **47**, 1674–1688.
9 A. Beyeler and P. Belser, *Coord. Chem. Rev.*, 2002, **230**, 29–39.
10 L. Friedman and F. M. Logullo, *J. Am. Chem. Soc.*, 1963, **85**, 1549–1549.
11 (*a*) T. Kitamura and M. Yamane, *J. Chem. Soc., Chem. Commun.*, 1995, 983–984; (*b*) T. Kitamura, M. Yamane, K. Inoue, M. Todaka, N. Fukatsu, Z. Meng and Y. Fujiwara, *J. Am. Chem. Soc.*, 1999, **121**, 11674–11679; (*c*) T. Kitamura, Z. Meng and Y. Fujiwara, *Tetrahedron Lett.*, 2000, **41**, 6611–6614; (*d*) T. Kitamura, M. Todaka and Y. Fujiwara, *Org. Synth.*, 2002, **78**, 104–108.
12 (*a*) A. Lorbach, C. Reus, M. Bolte, H.-W. Lerner and M. Wagner, *Adv. Synth. Catal.*, 2010, **352**, 3443–3449; (*b*) C. Reus, N.-W. Liu, M. Bolte, H.-W. Lerner and M. Wagner, *J. Org. Chem.*, 2012, **77**, 3518–3523.
13 K. Ma, M. Scheibitz, S. Scholz and M. Wagner, *J. Organomet. Chem.*, 2002, **652**, 11–19.
14 (*a*) F. Jäkle, T. Priermeier and M. Wagner, *J. Chem. Soc., Chem. Commun.*, 1995, 1765–1766; (*b*) F. Jäkle, T. Priermeier and M. Wagner, *Organometallics*, 1996, **15**, 2033–2040; (*c*) E. Herdtweck, F. Jäkle, G. Opromolla, M. Spiegler, M. Wagner and P. Zanello, *Organometallics*, 1996, **15**, 5524–5535; (*d*) E. Herdtweck, F. Jäkle and M. Wagner, *Organometallics*, 1997, **16**, 4737–4745.
15 (*a*) F. Fabrizi de Biani, T. Gmeinwieser, E. Herdtweck, F. Jäkle, F. Laschi, M. Wagner and P. Zanello, *Organometallics*, 1997, **16**, 4776–4787; (*b*) L. Ding, K. Ma, M. Bolte, F. Fabrizi de Biani, P. Zanello and M. Wagner, *J. Organomet. Chem.*, 2001, **637–639**, 390–397; (*c*) K. Ma, F. Fabrizi de Biani, M. Bolte, P. Zanello and M. Wagner, *Organometallics*, 2002, **21**, 3979–3989; (*d*) L. Ding, K. Ma, G. Dürner, M. Bolte, F. Fabrizi de Biani, P. Zanello and M. Wagner, *J. Chem. Soc., Dalton Trans.*, 2002, 1566–1573; (*e*) C. Cui, J. Heilmann-Brohl, A. Sánchez Perucha, M. D. Thomson, H. G. Roskos, M. Wagner and F. Jäkle, *Macromolecules*, 2010, **43**, 5256–5261.
16 (*a*) F. Jäkle, T. Priermeier and M. Wagner, *Chem. Ber.*, 1995, **128**, 1163–1169; (*b*) M. Fontani, F. Peters, W. Scherer, W. Wachter, M. Wagner and P. Zanello, *Eur. J. Inorg. Chem.*, 1998, 1453–1465; (*c*) M. Grosche, E. Herdtweck, F. Peters and M. Wagner, *Organometallics*, 1999, **18**, 4669–4672; (*d*) L. Ding, F. Fabrizi de Biani, M. Bolte, P. Zanello and M. Wagner, *Organometallics*, 2000, **19**, 5763–5768; (*e*) R. E. Dinnebier, M. Wagner, F. Peters, K. Shankland and W. I. F. David, *Z. Anorg. Allg. Chem.*, 2000, **626**, 1400–1405; (*f*) K. Ma, H.-W. Lerner, S. Scholz, J. W. Bats, M. Bolte and M. Wagner, *J. Organomet. Chem.*, 2002, **664**, 94–105.
17 W. Luo, L. N. Zakharov and S.-Y. Liu, *J. Am. Chem. Soc.*, 2011, **133**, 13006–13009.
18 For selected examples of B–N isosteres of aromatic molecules that give rise to new optoelectronic or biological properties, see: (*a*) A. J. Ashe III and X. Fang, *Org. Lett.*, 2000, **2**, 2089–2091; (*b*) A. J. Ashe III, X. Fang, X. Fang and J. W. Kampf, *Organometallics*, 2001, **20**, 5413–5418; (*c*) C. A. Jaska, D. J. H. Emslie, M. J. D. Bosdet, W. E. Piers, T. S. Sorensen and M. Parvez, *J. Am. Chem. Soc.*, 2006, **128**, 10885–10896; (*d*) M. J. D. Bosdet, W. E. Piers, T. S. Sorensen and M. Parvez, *Angew. Chem., Int. Ed.*, 2007, **46**, 4940–4943; (*e*) A. J. V. Marwitz, E. R. Abbey, J. T. Jenkins, L. N. Zakharov and S.-Y. Liu, *Org. Lett.*, 2007, **9**, 4905–4908; (*f*) Z. Liu and T. B. Marder, *Angew. Chem., Int. Ed.*, 2008, **47**, 242–244; (*g*) E. R. Abbey, L. N. Zakharov and S.-Y. Liu, *J. Am. Chem. Soc.*, 2008, **130**, 7250–7252; (*h*) A. J. V. Marwitz, M. H. Matus, L. N. Zakharov, D. A. Dixon and S.-Y. Liu, *Angew. Chem., Int. Ed.*, 2009, **48**, 973–977; (*i*) A. N. Lamm and S.-Y. Liu, *Mol. BioSyst.*, 2009, **5**, 1303–1305; (*j*) K. Raidongia, A. Nag, K. P. S. S. Hembram, U. V. Waghmare, R. Datta and C. N. R. Rao, *Chem.–Eur. J.*, 2010, **16**, 149–157; (*k*) T. Taniguchi and S. Yamaguchi, *Organometallics*, 2010, **29**, 5732–5735; (*l*) T. Hatakeyama, S. Hashimoto, S. Seki and M. Nakamura, *J. Am. Chem. Soc.*, 2011, **133**, 18614–18617; (*m*) P. G. Campbell, A. J. V. Marwitz and S.-Y. Liu, *Angew. Chem., Int. Ed.*, 2012, **51**, 6074–6092; (*n*) E. R. Abbey and S.-Y. Liu, *Org. Biomol. Chem.*, 2013, **11**, 2060–2069; (*o*) J.-S. Lu, S.-B. Ko, N. R. Walters, Y. Kang, F. Sauriol and S. Wang, *Angew. Chem., Int. Ed.*, 2013, **52**, 4544–4548.
19 A. Lorbach, M. Bolte, H.-W. Lerner and M. Wagner, *Chem. Commun.*, 2010, **46**, 3592–3594.
20 (*a*) D. N. Hendrickson, J. M. Hollander and W. L. Jolly, *Inorg. Chem.*, 1970, **9**, 612–615; (*b*) E. M. Holt, S. L. Holt, K. J. Watson and B. Olsen, *Cryst. Struct. Commun.*, 1978, **7**,

613–616; (*c*) D. C. Bradley, M. B. Hursthouse, J. Newton and N. P. C. Walker, *J. Chem. Soc., Chem. Commun.*, 1984, 188–190; (*d*) R. G. Ball, F. Edelmann, J. G. Matisons and J. Takats, *Inorg. Chim. Acta*, 1987, **132**, 137–143; (*e*) J. M. Boncella, M. L. Cajigal, A. S. Gamble and K. A. Abboud, *Polyhedron*, 1996, **15**, 2071–2078; (*f*) R. A. Kresiński, *J. Chem. Soc., Dalton Trans.*, 1999, 401–405; (*g*) C.-L. Lee, Y.-Y. Wu, C.-P. Wu, J.-D. Chen, T.-C. Keng and J.-C. Wang, *Inorg. Chim. Acta*, 1999, **292**, 182–188; (*h*) J.-C. Hierso and M. Etienne, *Eur. J. Inorg. Chem.*, 2000, 839–842; (*i*) C.-L. Lee, P.-Y. Yang, C.-W. Su, J.-D. Chen, L.-S. Liou and J.-C. Wang, *Inorg. Chim. Acta*, 2001, **314**, 147–153; (*j*) A. E. Enriquez, B. L. Scott and M. P. Neu, *Inorg. Chem.*, 2005, **44**, 7403–7413.

21 S. Trofimenko, *J. Am. Chem. Soc.*, 1969, **91**, 5410–5411.

22 J. Bielawski and K. Niedenzu, *Inorg. Chem.*, 1986, **25**, 85–87.

23 Ö. Seven, Z.-W. Qu, H. Zhu, M. Bolte, H.-W. Lerner, M. C. Holthausen and M. Wagner, *Chem.–Eur. J.*, 2012, **18**, 11284–11295.

24 M. Scheibitz, J. W. Bats, M. Bolte, H.-W. Lerner and M. Wagner, *Organometallics*, 2004, **23**, 940–942.

25 M. Scheibitz, H. Li, J. Schnorr, A. Sánchez Perucha, M. Bolte, H.-W. Lerner, F. Jäkle and M. Wagner, *J. Am. Chem. Soc.*, 2009, **131**, 16319–16329.

26 K. Niedenzu and H. Nöth, *Chem. Ber.*, 1983, **116**, 1132–1153.

27 S. Trofimenko, *Scorpionates - The Coordination Chemistry of Polypyrazolylborate Ligands*, Imperial College Press, London, 1999.

28 C. Pettinari, *Scorpionates II: Chelating Borate Ligands*, Imperial College Press, London, 2008.

29 H. Nöth and B. Wrackmeyer, in *Nuclear Magnetic Resonance Spectroscopy of Boron Compounds. NMR Basic Principles and Progress*, ed. P. Diehl, E. Fluck and R. Kosfeld, Springer, Berlin, 1978.

30 In most cases, we will give the smaller value for the angle between two planes as the interplanar/dihedral angle. The only exceptions are the angles between the blades of the B–N-triptycenes, for which we have chosen to consider the larger values, because throughout the literature angles close to 120° (instead of 60°) are given for triptycene.

31 K. Nikitin, C. Fleming, H. Müller-Bunz, Y. Ortin and M. J. McGlinchey, *Eur. J. Org. Chem.*, 2010, 5203–5216.

32 K. Anzenhofer and J. J. de Boer, *Z. Kristallogr.*, 1970, **131**, 103–113.

33 A. Pelter, K. Smith and H. C. Brown, *Borane Reagents*, Academic Press, London, 1988.

34 A. Lorbach, M. Bolte, H. Li, H.-W. Lerner, M. C. Holthausen, F. Jäkle and M. Wagner, *Angew. Chem., Int. Ed.*, 2009, **48**, 4584–4588.

35 H. Nöth and H. Vahrenkamp, *Chem. Ber.*, 1966, **99**, 1049–1067.

36 Similar results as for [**4b**]Br were obtained upon targeted methanolysis of [**4d**]Br, which gave the corresponding *syn* pyrazabole (*p*-$Me_3SiC_6H_4$)(CH_3O)B(μ-pz)$_2$B(OCH_3)(*p*-$C_6H_4SiMe_3$) (**12a**; *cf*. the ESI† for more information).

37 M. K. Das, A. L. DeGraffenreid, K. D. Edwards, L. Komorowski, J. F. Mariategui, B. W. Miller, M. T. Mojesky and K. Niedenzu, *Inorg. Chem.*, 1988, **27**, 3085–3089.

38 R. Chinchilla and C. Nájera, *Chem. Rev.*, 2007, **107**, 874–922.

39 J. K. Stille, *Angew. Chem., Int. Ed. Engl.*, 1986, **25**, 508–524.

40 P. Espinet and A. M. Echavarren, *Angew. Chem., Int. Ed.*, 2004, **43**, 4704–4734.

41 Ö. Seven, M. Bolte, H.-W. Lerner and M. Wagner, *Organometallics*, 2014, **33**, 1291–1299.

42 S. Trofimenko, *J. Am. Chem. Soc.*, 1967, **89**, 3170–3177.

43 J. Zagermann, M. C. Kuchta, K. Merz and N. Metzler-Nolte, *Eur. J. Inorg. Chem.*, 2009, 5407–5412.

44 S. Popp, K. Ruth, H.-W. Lerner and M. Bolte, *Acta Crystallogr., Sect. C: Cryst. Struct. Commun.*, 2012, **68**, o226–o230.

45 M. I. Rodríguez-Franco, I. Dorronsoro, A. I. Hernández-Higueras and G. Antequera, *Tetrahedron Lett.*, 2001, **42**, 863–865.

46 I. Meana, A. C. Albéniz and P. Espinet, *Adv. Synth. Catal.*, 2010, **352**, 2887–2891.

47 L. Birkofer and M. Franz, *Chem. Ber.*, 1972, **105**, 1759–1767.

48 C. Fernández-Castaño, C. Foces-Foces, N. Jagerovic and J. Elguero, *J. Mol. Struct.*, 1995, **355**, 265–271.

49 A. L. Spek, *J. Appl. Crystallogr.*, 2003, **36**, 7–13.

50 Stoe & Cie, *X-AREA. Diffractometer control program system*, Stoe & Cie, Darmstadt, Germany, 2002.

51 G. M. Sheldrick, *Acta Crystallogr., Sect. A: Found. Crystallogr.*, 2008, **64**, 112–122.